Contribution of Imaging to Organs at Risk Dose during Lung Stereotactic Body Radiation Therapy

Milovan Savanović[1,2]*⑩, François Gardavaud[3], Dražan Jaroš[4], Bénédicte Lonkuta[5], Matthias Barral[6], François Henri Cornelis[7], Jean-Noël Foulquier[8]

ABSTRACT

Background: The use of imaging is indispensable in modern radiation therapy, both for simulation and treatment delivery. For safe and sure utilization, dose delivery from imaging must be evaluated.

Objective: This study aims to investigate the dose to organ at risk (OAR) delivered by imaging during lung stereotactic body radiation therapy (SBRT) and to evaluate its contribution to the treatment total dose.

Material and Methods: In this retrospectively study, imaging total dose to organs at risk (OARs) (spinal cord, esophagus, lungs, and heart) and effective dose were retrospectively evaluated from 100 consecutive patients of a single institution who had lung SBRT. For each patient, dose was estimated using Monte-Carlo convolution for helical computed tomography (helical CT), Four-Dimensional CT (4D-CT), and kilovoltage Cone-Beam CT (kV-CBCT). Helical CT and kV-CBCT dose were evaluated for the entire thorax acquisition, while 4D-CT dose was analyzed on upper lobe (UL) or lower lobe (LL) acquisition. Treatment dose was extracted from treatment planning system and compared to imaging total dose.

Results: Imaging total dose maximum values were 117 mGy to the spinal cord, 127 mGy to the esophagus, 176 mGy to the lungs and 193 mGy to the heart. The maximum effective dose was 19.65 mSv for helical CT, 10.62 mSv for kV-CBCT, 25.95 mSv and 38.45 mSv for 4D-CT in UL and LL regions, respectively. Depending on OAR, treatment total dose was higher from 1.7 to 8.2 times than imaging total dose. Imaging total dose contributed only to 0.3% of treatment total dose.

Conclusion: Imaging dose delivered with 4D-CT to the OARs is higher than those of others modalities. The heart received the highest imaging dose for both UL and LL. Total imaging dose is negligible since it contributed only to 0.3% of treatment total dose.

Introduction

Stereotactic Body Radiation Therapy (SBRT) of lung cancer uses high doses delivered into a tumor in few fractions [1]. Since SBRT uses high doses, it is necessary to minimize treatment uncertainties performing conformal targeting, precise tumor and organ delineation, and patient positioning to ensure tumor local control and to limit

[1]PhD Candidate, Department of Radiation Oncology, Tenon Hospital, 75020 Paris, France
[2]PhD Candidate, Faculty of Medicine, University of Paris-Saclay, 94276 Le Kremlin-Bicêtre, France
[3]PhD Candidate, Department of Radiology, Tenon Hospital, 75020 Paris, France
[4]PhD Candidate, Affidea, International Medical Centers, Center for Radiotherapy, 78000 Banja Luka, Bosnia and Herzegovina
[5]MSc, Department of Radiology, Tenon Hospital, 75020 Paris, France
[6]MD, Department of Radiology, Tenon Hospital, 75020 Paris, France
[7]PhD, Department of Radiology, Tenon Hospital, 75020 Paris, France
8PhD, Department of Radiation Oncology, Tenon Hospital, 75020 Paris, France

*Corresponding author:
Milovan Savanovic
Department of Radiation Oncology, Tenon Hospital, 75020 Paris, France
E-mail: milovan_savanovic@yahoo.com

organs at risk (OAR) radiation exposure. In lung SBRT, the computed tomography (CT) in helical mode (helical CT) and Four-Dimensional CT (4D-CT) are used during simulation [2]. To ensure patient positioning during treatment delivery, kilovoltage Cone-Beam CT (kV-CBCT) is recommended to reduce uncertainties due to patient positioning, inter- and intra-fraction motion [3-5].

However, image guidance has an important role in improving SBRT safety and efficacy, it could yield to expose OARs outside the therapeutic beams [6, 7]. If significant image guidance dose (generally using MV imaging) can theoretically have an impact on tumor and OARs biological effects such as local control, necrosis or tissue damage [8-11]. kV imaging may increase the secondary cancer risk, particularly for organs outside the treatment field [12-14]. According to the American Association of Physics in Medicine (AAPM), imaging dose should be included in the treatment planning when superior to 5 % of planned dose [6]. It requires to consider dose calculation and delivery accuracy, tumor-to-organ proximity, dose tolerances for critical organs, treatment technique and feasibility in clinical practice to ensure tumor local control and better sparing of OARs [6].

Only three studies, two with kV-CBCT and one with 4D-CT, have evaluated imaging dose with adult patients with lung cancer [15-17]. In the present study, patient-specific imaging dose was evaluated for lung SBRT, including dose delivered during simulation using helical CT and 4D-CT, and before each fraction of treatment delivery using kV-CBCT [18]. The purpose of this study was to investigate the dose to OAR delivered by imaging during lung SBRT and to evaluate its contribution to the treatment total dose.

Material and Methods

Patient selection
In this retrospectively study, a total of 100

patients, with small tumor size (≤ 5 cm) who had lung SBRT, were included. The patients' characteristics are presented in Table 1.

All patients were enrolled in an Institutional Review Board approved protocol. This protocol was Health Insurance Portability and Accountability Act compliant.

CT acquisitions and dose calculation
During simulation for lung SBRT, patients were positioned in the supine position with arms above the head using the BlueBAG BodyFIX system immobilization (Medical Intelligence, Schwabmünchen, Germany). All patients were scanned on 16 slices CT scan (GE Lightspeed, General Electric Medical Systems, Waukesha, WI, USA), equipped with the Real-time Positioning Management system (RPM, Varian Medical Systems, Palo Alto, CA, USA). From Institutional protocol,

Table 1: Patient characteristics

Characteristics	Raw data
Number of patients	100
Age	70 (38 – 90)
Gender	
Male	58
Female	42
Tumor location	
Upper lobe	68
Lower lobe	32
Tumor size	
Upper lobe (mm)	32 (17 – 50)
Lower lobe (mm)	37 (21 – 49)
Weight (kg)	63.5 (39.0 – 106.0)
Height (m)	1.68 (1.48 – 1.86)
BMI (kg/m²)	23.0 (15.2 – 35.9)
Breathing cycle (s)	4.3 (1.7 – 9.6)
4D-CT scan time (s)	54 (29 – 94)
Number of fractions	5 (4 – 8)

BMI: Body mass index, 4D-CT: Four-Dimensional Computed Tomography

two helical scans were performed, followed by one 4D-CT scan. The CT parameters used during clinical acquisitions are presented in (Table 2).

For the helical scans, acquisition was performed from the cricoid cartilage to the second lumbar vertebra (Figure 1(a)), while 4D-CT acquisition was performed with fifteen slices below and above tumor localization (in the upper lobe (UL) Figure 1 (b) and the lower lobe (LL) region Figure 1 (c)).

For all CT acquisitions, volume computed tomography dose index (CTDI$_{vol}$) has been extracted automatically from DICOM images using dedicated home-made scripts in MATLAB R2020a (MathWorks, Natick, Massachusetts).

Dose to OARs (spinal cord, esophagus, lungs, heart) was calculated for each patient (see patient anatomical attributes in Table 1) with CT scans parameters (Table 2), in the UL and LL (Figure 2) using the National Cancer Institute dosimetry system for CT (NCICT

Table 2: Parameters of helical computed tomography (CT) and Four-Dimensional Computed Tomography (4D-CT) acquisitions

Parameters	Helical CT	4D-CT
Rotation time (s)	0.7	0.7
Pitch	0.938	/
Images per rotation	/	16
Collimation (mm)	20	20
Slice thickness (mm)	1.25	1.25
SFOV	Large Body	Large Body
kV	120	120
mA min	10	10
mA max	440	440
Noise index	9.83	9.83
AutomA/smartmA	Yes / Yes	Yes / Yes

CT: Computed tomography, 4D-CT: Four-Dimensional Computed Tomography, SFOV: Scan field of view, kV: kilo voltage, min mA: minimum value of milliampere modulation, max mA: maximum value of milliampere modulation
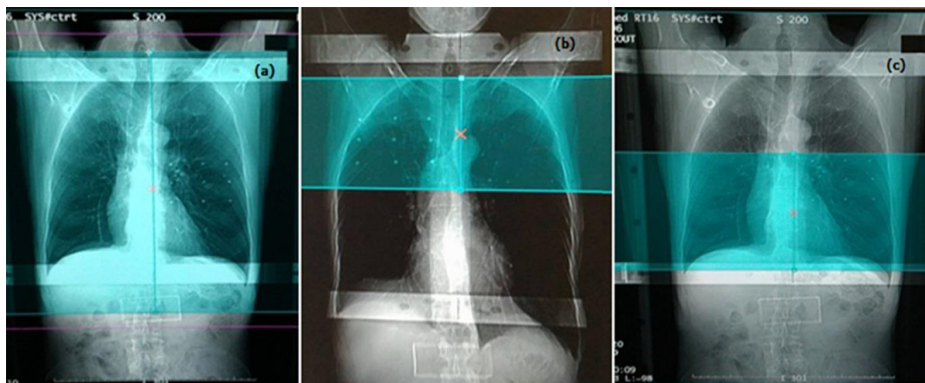

Figure 1: Scan area (in blue box) for helical computed tomography (CT) (a), Four-Dimensional Computed Tomography (4D-CT) acquisition for tumor located in the upper lobe (UL) (b), and 4D-CT acquisition for tumor located in the lower lobe (LL) (c)
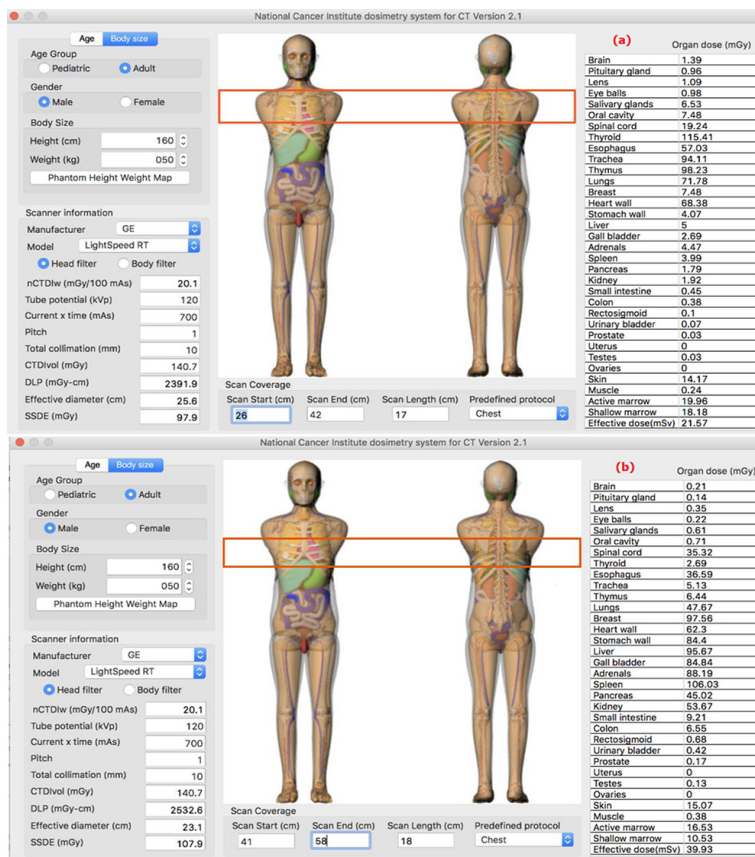
National Cancer Institute dosimetry system for CT Version 2.1

(a)

Organ	dose (mGy)
Brain	1.39
Pituitary gland	0.96
Lens	1.09
Eye balls	0.98
Salivary glands	6.53
Oral cavity	7.48
Spinal cord	19.24
Thyroid	115.41
Esophagus	57.03
Trachea	94.11
Thymus	98.23
Lungs	71.78
Breast	7.48
Heart wall	68.38
Stomach wall	4.07
Liver	5
Gall bladder	2.69
Adrenals	4.47
Spleen	3.99
Pancreas	1.79
Kidney	1.92
Small intestine	0.45
Colon	0.38
Rectosigmoid	0.1
Urinary bladder	0.07
Prostate	0.03
Uterus	0
Testes	0.03
Ovaries	0
Skin	14.17
Muscle	0.24
Active marrow	19.96
Shallow marrow	18.18
Effective dose(mSv)	21.57

Scanner information: Manufacturer GE; Model LightSpeed RT; Head filter; nCTDIw (mGy/100 mAs) 20.1; Tube potential (kVp) 120; Current x time (mAs) 700; Pitch 1; Total collimation (mm) 10; CTDIvol (mGy) 140.7; DLP (mGy-cm) 2391.9; Effective diameter (cm) 25.6; SSDE (mGy) 97.9

Scan Coverage: Scan Start (cm) 26; Scan End (cm) 42; Scan Length (cm) 17; Predefined protocol Chest

National Cancer Institute dosimetry system for CT Version 2.1

(b)

Organ	dose (mGy)
Brain	0.21
Pituitary gland	0.14
Lens	0.35
Eye balls	0.22
Salivary glands	0.61
Oral cavity	0.71
Spinal cord	35.32
Thyroid	2.69
Esophagus	36.59
Trachea	5.13
Thymus	6.44
Lungs	47.67
Breast	97.56
Heart wall	62.3
Stomach wall	84.4
Liver	95.67
Gall bladder	84.84
Adrenals	88.19
Spleen	106.03
Pancreas	45.02
Kidney	53.67
Small intestine	9.21
Colon	6.55
Rectosigmoid	0.68
Urinary bladder	0.42
Prostate	0.17
Uterus	0
Testes	0.13
Ovaries	0
Skin	15.07
Muscle	0.38
Active marrow	16.53
Shallow marrow	10.53
Effective dose(mSv)	39.93

Scanner information: Manufacturer GE; Model LightSpeed RT; Head filter; nCTDIw (mGy/100 mAs) 20.1; Tube potential (kVp) 120; Current x time (mAs) 700; Pitch 1; Total collimation (mm) 10; CTDIvol (mGy) 140.7; DLP (mGy-cm) 2532.6; Effective diameter (cm) 23.1; SSDE (mGy) 107.9

Scan Coverage: Scan Start (cm) 41; Scan End (cm) 58; Scan Length (cm) 18; Predefined protocol Chest

Figure 2: National Cancer Institute dosimetry system for CT (NCICT) software Graphical User Interface (GUI) calculating dose delivered by Four-Dimensional Computed Tomography (4D-CT) to organs at risk (OARs) in the scan area illustrated with the red rectangle for upper lobe (UL) (a) and lower lobe (LL) regions (b)

v2.1, NIH, Bethesda, Maryland, USA) based on Monte-Carlo convolution [19]. Helical CT dose simulated in NCICT included the complete thorax (Figure 1 (a)), whereas 4D-CT examination scan area depends on tumor location: UL or LL (Figure 2). The scanned region size was different for each patient (in regard of the tumor size) and the patient body habitus was tailored for each patient in NCICT thanks to the International Commission on Radiological Protection (ICRP) reference adult phantoms [20, 21]. All the scan parameters displayed in Table 1 were implemented in NCICT software to determine organ dose exposure, except for tube current modulation (TCM) where the miliAmpere mean value, specific for each exam. This was retained since NCICT v2.1 does not offer an accessible option in the Graphical User Interface (GUI) to take into account TCM mode.

kV-CBCT acquisitions and dose calculation

During treatment delivery with a Novalis TrueBeam STx (Varian Medical System, Palo Alto, CA, USA), the patient positioning was verified using kV-CBCT scan. The kV-CBCT images were acquired with half-fan full scan mode (360°), 125 kV, 270 mAs, 14° anode angle, field size 20 cm × 26.5 cm, 900 projections and 60 s for the exposure time. For all kV-CBCT acquisitions, volume computed tomography dose index (CTDI$_{vol}$) has been extracted automatically from DICOM images using dedicated home-made scripts in MATLAB R2020a (MathWorks, Natick, Massachusetts).

To measured air kerma, the half-value layer

(HVL) and the beam filtration, Black Piranha detector (RTI Electronics Inc, NJ, USA) was used. Then a Monte Carlo program for calculating patient organ doses in medical x-ray examinations (PCXMC v2.0, Stuk, Helsinki, Finland) was used in batch mode to compute dose delivered to the OARs from kV-CBCT acquisitions [22]. Each patient body habitus has been tailored in PCXMC software.

Calculation of total exposure from imaging acquisitions

Imaging total dose delivered to the OARs is calculated as a total sum of doses delivered to the OARs from all modalities: helical CT scan, 4D-CT scan and kV-CBCT during lung SBRT treatment. For the helical CT and kV-CBCT scans, imaging dose evaluation was performed for the entire thorax, while imaging dose from 4D-CT was evaluated for specific scanned regions such as UL or LL (red rectangles in Figure 2).

Imaging total dose was calculated based on institutional protocol, by summing doses from two helical CT scans, one cine 4D-CT and five kV-CBCT (five being the mean value of all fractions).

Imaging total dose delivered to one organ was presented by equation (1):

$$D_t\left(organ_i\right) = \left(a \times D_{hCT}\left(organ_i\right)\right) + D_{4D\text{-}CT}\left(organ_i\right) + \left(b \times D_{CBCT}\left(organ_i\right)\right) (1)$$

Where $D_t(organ_i)$ –imaging total dose delivered to the organ of interest, a – number of helical CT sequences, $D_{hCT}(organ_i)$ – dose delivered by helical CT to the organ of interest, $D_{4D\text{-}CT}(organ_i)$ – dose delivered by 4D-CT to the organ of interest, b – number of CBCT sequences, $D_{CBCT}(organ_i)$ – dose delivered by CBCT to the organ of interest.

For each OAR, the maximum value of imaging total dose has been computed.

Treatment planning and dose constraints

Lung SBRT plans were performed on the helical CT scan without stereotactic body frame with two to four partial dynamic conformal arcs (DCAs) using 6 MV beams. The treat-ment dose was 60 Gy in 4 to 8 fractions prescribed to isodose line 80%. Treatment planning was performed with the Pinnacle Version 9.10 (Koninklijke Philips N.V., Amsterdam, Netherlands) treatment planning system (TPS) and calculated using the Collapsed Cone Convolution (CCC) algorithm [23, 24]. The constraints for the planning target volume (PTV) coverage were D98%>95% and D95%≥100%. The OARs constraints were based on ICRU 91 report recommendations using maximum dose (D_{max}) which should be less than 15 Gy (0.1 cc) for the spinal cord, 30 Gy (0.5 cc) for the heart and 27 Gy (0.5 cc) for the esophagus [25]. For the lungs volume, where the PTV had been subtracted (Lungs-PTV), two constraints were established. The percentage volume receiving 20 Gy or more (V_{20}) and 16 Gy or more (V_{16}) was restricted to 10 % and 20 % of the prescribed dose respectively.

Dose-volume histograms (DVH) were generated for the PTV and all OARs. OARs doses were evaluated using mean dose (D_{mean}) and D_{max}, respectively. Doses delivered to the OARs were manually extracted from DVHs for all 100 patients.

Data analysis

Statistical analysis and violin plots computation of doses delivered to the OARs (spinal cord, esophagus, lungs and heart) from imaging chain were evaluated using GraphPad Prism 8.1.2 version (SD, California, USA). To compare results between all modalities, Kruskal Wallis test was used. The imaging maximum total dose has been compared to the treatment total dose using paired t-test. Data was considered statistically significant at p < 0.05.

Results

The mean values of the $CTDI_{vol}$ obtained were 23.1 ± 3.8 mGy and 55.6 ± 13.3 mGy (p<0.0001) during helical CT and cine 4D-CT scans, respectively, while $CTDI_{vol}$ from kV-CBCT remained constant at 4 mGy. Air kerma

mean value was 13.8 ± 0.3 mGy. Mean half-value layer was 4.88 ± 0.01 mmAl and mean beam filtration was 10.12 ± 0.01 mmAl. Imaging mean dose delivered to the OARs and associated effective dose are presented in Table 3. Results presented in Table 3 were all statistically significant (p < 0.01).

Imaging doses maximum values delivered to the OARs from helical CT, kV-CBCT and 4D-CT in the UL and LL area were, respectively: 19.52 mGy, 9.74 mGy, 37.76 mGy and 36.89 mGy to the spinal cord; 29.74 mGy, 5.03 mGy, 56.69 mGy and 36.95 mGy to the esophagus; 40.01 mGy, 6.32 mGy, 83.48 mGy and 50.58 mGy to the lung; 41.05 mGy, 9.13 mGy, 68.60 mGy and 66.66 mGy to the heart.

Imaging total dose maximum values were 117 mGy to the spinal cord, 127 mGy to the esophagus, 176 mGy to the lungs and 193 mGy to the heart.

The maximum effective dose was 19.65 mSv for helical CT, 10.62 mSv for kV-CBCT, 25.95 mSv and 38.45 mSv for 4D-CT in UL and LL regions, respectively.

The highest imaging doses were delivered to the heart (41.05 mGy) for helical CT (p<0.0001), to the spinal cord (9.74 mGy) for kV-CBCT (p<0.0001), to the lung (83.48 mGy) for 4D-CT in UL region (p<0.0001) and to the heart (68.60 mGy) for 4D-CT in LL re-

gion (p<0.0001).

Imaging doses delivered to the OARs (spinal cord, esophagus, lungs and heart) were presented in Figure 3.

The PTV coverage (D98%>95% was 98.5±0.6 % and D95%≥100%100.06±1.1 %) yields to OARs doses. Mean doses (D_{mean}) and maximum doses (D_{max}) in volume (0.1 cc for the spinal cord and 0.5 cc for the heart and esophagus) delivered to the OARs were presented depending on the lobe (UL and LL regions) in Table 4.

Comparison of treatment beam mean doses with imaging total mean dose, depending on UL and LL regions, was presented in Table 5 with associated relative gap rations (RGR) and p-values.

Discussion

Imaging total dose was evaluated as the sum of the doses delivered to the OARs from two helical CT scans, one 4D-CT scan and five kV-CBCT acquisitions. Imaging maximum total dose was delivered to the heart (193 mGy), then to the lungs (176 mGy), the esophagus (127 mGy) and the spinal cord (117 mGy). These doses are negligible comparing to the total dose delivered during SBRT treatment for lung cancer. Indeed, imaging total dose contributed up to only 0.3 % of 60 Gy of the treat-

Table 3: Mean values and standard deviation of the dose delivered to the organs at risk (OARs), effective dose and imaging total dose were evaluated from different modalities depending on scanned regions

Technique	Zone	Spinal cord (mGy)	Esophagus (mGy)	Lungs (mGy)	Heart (mGy)	D_{eff} (mSv)
Helical CT	WT	11.54±3.05	21.08±4.30	29.02±5.40	29.40±5.76	14.29±2.43
kV-CBCT	WT	7.14±1.46	3.52±1.66	4.50±2.11	6.86±2.41	1.33±0.63
4D-CT	UL	11.80±5.40	32.07±8.19	46.45±12.67	38.44±12.07	13.93±4.11
	LL	17.77±6.64	21.67±6.77	30.20±9.42	39.69±12.46	22.43±6.04
Total	UL	74.40±15.72	94.47±13.87	130.14±19.19	135.97±20.89	50.28±6.62
	LL	77.26±16.59	80.29±14.77	109.57±18.67	131.91±23.59	56.95±8.66

CT: Computed tomography, kV-CBCT: kilovoltage Cone-Beam computed tomography, 4D-CT: Four-Dimensional Computed Tomography, WT: Whole thorax, UL: Upper lobe, LL: Lower lobe, mGy: milli-gray, D_{eff}: Effective dose
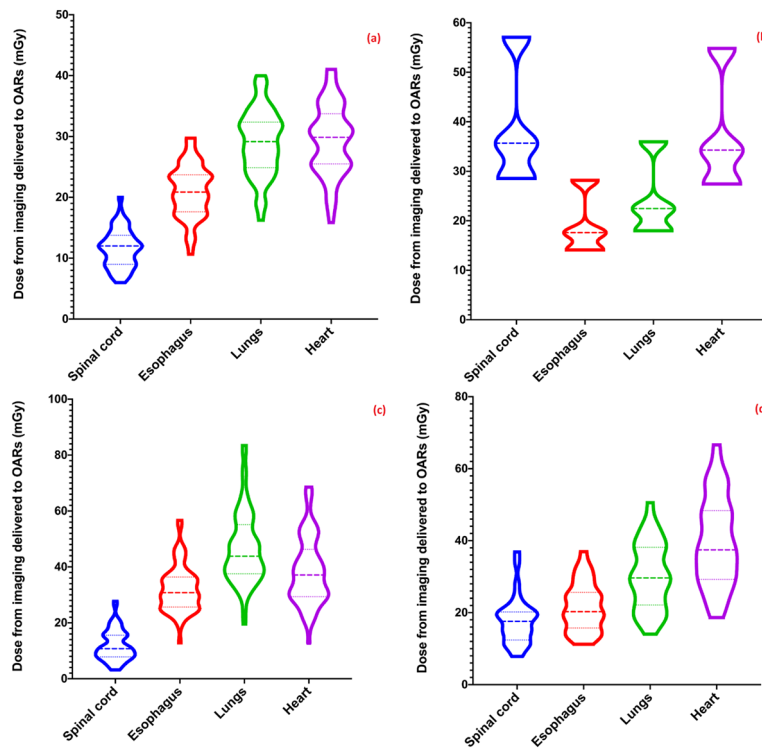
Figure 3: Violin plots of dose delivered to the organs at risk (OARs) evaluated from Helical computed tomography (CT) from whole thorax (a); kilovoltage Cone-Beam CT (kV-CBCT) from whole thorax (b); cine Four-Dimensional Computed Tomography (4D-CT) in upper lobe (UL) region (c); and cine 4D-CT in lower lobe (LL) area (d). The dashed lines near the middle of the plots indicate the medians and the dot lines indicate the quartiles

Table 4: The results of mean doses and maximum doses in volume (0.1 cc for the spinal cord and 0.5 cc for the heart and esophagus) evaluated from treatment planning system (TPS) for the spinal cord, esophagus, lungs and heart, depending on the lobe (upper lobe (UL) and lower lobe (LL) regions)

Lobe	Dose	Spinal cord	Esophagus	Lungs		Heart
				$V_{20}<10\ \%$	$V_{16}<20\ \%$	
UL	D_{mean} (Gy)	1.24±0.93	2.84±2.42	3.49±1.84	6.05±3.96	0.93±1.86
	D_{max} (Gy)	10.19±6.31	14.93±11.97	4.62±3.13		8.74±16.18
LL	D_{mean} (Gy)	1.54±1.27	2.52±1.33	3.88±2.37	6.84±4.42	3.27±3.35
	D_{max} (Gy)	11.02±6.20	10.94±3.64	5.11±3.46		16.54±14.51

UL: Upper lobe, LL: Lower lobe, D_{mean}: mean dose, D_{max}: maximum dose

ment total dose delivered. It is worth to consider that imaging total dose delivered to the OARs is insufficient to impact on tumor local control (necrosis) and/or OARs damage, because it represents less than 5 % of prescribed treatment dose according to AAPM [6]. This result is comparable with data currently available in the literature which indicates that imaging dose during image guidance is generally less than 5% of the therapeutic target dose

Table 5: Comparison between treatment beam mean doses and imaging total mean dose delivered to the organs at risk (OARs) depending on upper lobe (UL) and lower lobe (LL) areas with associated relative gap rations and p-values were presented

OARs	Upper lobe				Lower lobe			
	TPS	Imaging	RGR	p	TPS	Imaging	RGR	p
	(mGy)	(mGy)			(mGy)	(mGy)		
Sc	1240±930	74.4±15.7	16.7	<0.0001	11020±6200	77.3±16.6	121	<0.0001
Esophagus	2840±2420	94.5±13.9	30.1	<0.0001	10940±3640	80.3±14.8	137.6	<0.0001
Lung	3490±760	130.1±19.2	26.8	<0.0001	6840±4420	109.6±18.7	52.9	<0.0001
Heart	930±1840	136.0±20.9	6.8	<0.0001	16540±14510	131.9±23.6	106.9	<0.0001

OARs: Organs at risk, Sc: Spinal cord, TPS: Treatment planning system, RGR: Relative GAP

[26-28].

However, as demonstrated in this study, dose delivered to the OARs depends on imaging modality. Highest doses were delivered to the heart from the helical CT (p<0.0001), to the spinal cord from the kV-CBCT (p<0.0001), to the lungs in UL region from 4D-CT (p<0.0001), and to the heart in LL region from 4D-CT (p<0.0001). As the heart is located in chest middle, it was the most exposed organ for helical CT, 4D-CT in LL area and for the imaging total dose. For the same reason, it was also the second most exposed for kV-CBCT (after spinal cord) and for 4D-CT in the UL (after lungs). The highest dose delivered to the spinal cord from kV-CBCT was due to sequential acquisition technique without cradle displacement contrary to helical CT acquisition which involves cradle displacement. Lungs were the most exposed organ in the UL from 4D-CT due to larger exposed volume than the heart (Figure 1).

In the meantime, higher dose was delivered to the OARs with 4D-CT than helical CT. Comparing helical CT vs 4D-CT acquisitions, higher dose in UL region was delivered with 4D-CT to the esophagus (32 %), to the lung (33 %) and to the heart (20 %), while helical CT was delivered higher dose to the spinal cord (9 %) than 4D-CT. In LL region, 4D-CT was delivered higher dose to the spinal cord (33 %) than helical CT, while helical CT was

delivered higher dose to the heart (20 %). A smaller difference between dose delivered to the esophagus (3 %) and lung (2 %) was found comparing helical CT vs 4D-CT in LL area. These doses differences from several modalities could be explained by the fact that the helical CT was performed for the whole thorax region, while 4D-CT was performed on a tailored area depending on tumor localization (UL and LL) (Figure 1). In Yang et al. study, doses to OARs were compared between helical CT scan versus 4D-CT scan [17]. They reported that higher doses were delivered to OARs using 4D-CT compared to helical CT: heart 8.0 vs 103.0 mGy; bilateral lungs 7.1 vs 94.6 mGy; spinal cord 7.4 vs 94.2 mGy; esophagus 7.9 vs 103.7 mGy [17]. Compared to the results from the Yang et al. study, higher doses were delivered to the OARs (from 1.5 to 3.5 times) for the helical CT, while lower doses were delivered to the OARs (from 2 to 5 times) for 4D-CT in this study [17]. These differences were provided from different manufactured CT scans, acquisition parameters (helical CT and 4D-CT) and scanned regions (4D-CT) in this study, compared to the previously cited study [17].

Comparing helical CT versus kV-CBCT, dose delivered to the OARs was higher using helical CT: 1.7 times to the spinal cord, 5.9 times to esophagus, 6.5 times to the lungs, 4.4 times to the heart. Helical CT delivered

higher effective dose (10.7 times higher) than kV-CBCT. Spezi et al. evaluated dose to the lung and spinal cord from six chest cases using the X-ray volume imaging unit mounted on an Elekta Synergy linear accelerator (Elekta, Crawley, UK) [15]. They reported that dose delivered to the lung and spinal cord was less than 40 and 50 mGy, respectively [15]. In Nakamura et al. study, imaging mean doses were less than 26 mGy for soft tissues (such as lung, spinal cord and heart) from 3D-CBCT scans for nine lung cancer patients [16]. These OARs received slightly higher mean doses in these previous studies due to differences between their imaging acquisition parameters and those of this study [16].

This study has several limitations. Thus, therapeutic doses were compared to imaging dose by mean values instead of maximum values because commercial imaging dosimetric simulation software did not allow users to perform dose computation on each phantom voxels. In these imaging dosimetric software, only the mean dose was available. Finally, biological effects on exposed organs between low energy (kV) and high energy (MV) could be different as this depends on the secondary electrons range. In the diagnostic imaging field, the secondary electrons range is short due to low energies. At a megavoltage photon beam, the secondary electrons range increases leading to regions where dose buildup is not in electronic equilibrium and thus raises biological risk [29].

Conclusion

In conclusion, imaging exposure depends on acquisition parameters specific to each imaging modality. OARs exposure was higher using 4D-CT than other imaging modalities and depends on tumor size and location. The imaging maximum total dose compared to total dose delivered from lung SBRT treatment (0.3 %) was below the AAPM recommended threshold (5 %) and could not be included in treatment planning.

Conflict of Interest

None

References

1. Abreu CE, Ferreira PP, De Moraes FY, et al. Stereotactic body radiotherapy in lung cancer: an update. *J Bras Pneumol.* 2015;**41**(4):376-87. doi: 10.1590/S1806-37132015000000034. PubMed PMID: 26398758. PubMed PMCID: PMC4635958.

2. Lambrecht M, Sonke JJ, Nestle U, et al. Quality assurance of four-dimensional computed tomography in a multicentre trial of stereotactic body radiotherapy of centrally located lung tumours. *Phys Imag Radiat Oncol.* 2018;**8**:57-62. doi: 10.1016/j.phro.2018.10.003.

3. Molitoris JK, Diwanji T, Snider III JW, et al. Optimizing immobilization, margins, and imaging for lung stereotactic body radiation therapy. *Transl Lung Cancer Res.* 2019;**8**(1):24-31. doi: 10.21037/tlcr.2018.09.25. PubMed PMID: 30788232. PubMed PMCID: PMC6351403.

4. Srinivasan K. Mohammadi M. Shepherd J. Applications of linac-mounted kilovoltage Cone-beam Computed Tomography in modern radiation therapy: A review. *Pol J Radiol.* 2014;**79**:181-93. doi: 10.12659/PJR.890745. PubMed PMID: 25006356. PubMed PMCID: PMC4085117.

5. Goyal S. Kataria T. Image guidance in radiation therapy: techniques and applications. *Radiol Res Pract.* 2014;**2014**:1-10. doi: 10.1155/2014/705604. PubMed PMID: 25587445. PubMed PMCID: PMC4281403.

6. Ding GX, Alaei P, Curran B, et al. Image guidance doses delivered during radiotherapy: Quantification, management, and reduction: Report of the AAPM Therapy Physics Committee Task Group 180. *Med Phys.* 2018;**45**(5):e84-99. doi: 10.1002/mp.12824. PubMed PMID: 29468678.

7. Guckenberger M, Meyer J, Wilbert J, et al. Cone-beam CT based image-guidance for extracranial stereotactic radiotherapy of intrapulmonary tumors. *Acta Oncol.* 2006;**45**(7):897-906. doi: 10.1080/02841860600904839. PubMed PMID: 16982556.

8. Brahme A. Dosimetric precision requirements in radiation therapy. *Acta Radiol Oncol.* 1984;**23**:379-91. doi: 10.3109/02841868409136037. PubMed PMID: 6095609.

9. Dutreix A. When and how can we improve precision in radiotherapy? *Radiother Oncol.* 1984;**2**:275-92. doi: 10.1016/S0167-8140(84)80070-5.

10. Wambersie A. What accuracy is required and can be achieved in radiation therapy (review of radiobiological and clinical data). *Radiochim Acta.*

2001;**89**:255-64. doi: 10.1524/ract.2001.89.4-5.255.

11. Herring DF. The degree of precision required in the radiation dose delivered in cancer radiotherapy. Proc. 3rd ICCR, 1970 British institute of radiology special report; Glasgow, Scotland: British Institute of Radiology; 1971. p. 51-8.

12. Dzierma Y, Mikulla K, Richter P, et al. Imaging dose and secondary cancer risk in image-guided radiotherapy of pediatric patients. *Radiat Oncol.* 2018;**13**(1):168. doi: 10.1186/s13014-018-1109-8.

13. Zhou L, Bai S, Zhang YB, et al. Imaging Dose, Cancer Risk and Cost Analysis in Image-guided Radiotherapy of Cancers. *Scientific Reports*. 2018;8(1):10076. doi: 10.1038/s41598-018-28431-9.

14. Dong Wook K, Weon C, Myonggeun Y. Imaging Doses and Secondary Cancer Risk From Kilovoltage Cone-beam CT in Radiation Therapy. *Health Physics.* 2013;**104**:499-503. doi: 10.1097/HP.0b013e318285c685. PubMed PMID: 23532078.

15. Spezi E, Downes P, Jarvis R, et al. Patient-specific three-dimensional concomitant dose from cone beam computed tomography exposure in image-guided radiotherapy. *Int J Radiat Oncol Biol Phys.* 2012;**83**(1):419-26. doi: 10.1016/j.ijrobp.2011.06.1972. PubMed PMID: 22027261.

16. Nakamura M, Ishihara Y, Matsuo Y, et al. Quantification of the kV X-ray imaging dose during real-time tumor tracking and from three- and four-dimensional cone-beam computed tomography in lung cancer patients using a Monte Carlo simulation. *J Radiat Res.* 2018;**59**(2):173-81. doi: 10.1093/jrr/rrx098. PubMed PMID: 29385514. PubMed PMCID: PMC5950977.

17. Yang C, Liu R, Ming X, Liu N, Guan Y, Feng Y. Thoracic Organ Doses and Cancer Risk from Low Pitch Helical 4-Dimensional Computed Tomography Scans. *Biomed Res Int.* 2018;**2018**:8927290. doi: 10.1155/2018/8927290. PubMed PMID: 30345309. PubMed PMCID: PMC6174794.

18. Li R, Han B, Meng B, et al. Clinical implementation of intrafraction cone beam computed tomography imaging during lung tumor stereotactic ablative radiation therapy. *Int J Radiat Oncol Biol Phys.* 2013;**87**(5):917-23. doi: 10.1016/j.ijrobp.2013.08.015. PubMed PMID: 24113060. PubMed PMCID: PMC3888501.

19. Lee C, Kim KP, Bolch WE, Moroz BE, Folio L. NCICT: a computational solution to estimate organ doses for pediatric and adult patients undergoing CT scans. *J Radiol Prot.* 2015;**35**:891-909. doi: 10.1088/0952-4746/35/4/891. PubMed PMID: 26609995.

20. Menzel HG, Clement C, DeLuca P. ICRP Publication 110. Realistic reference phantoms: an ICRP/ICRU joint effort. A report of adult reference computational phantoms. *Ann ICRP.* 2009;**39**(2):1-164. doi: 10.1016/j.icrp.2009.09.001. PubMed PMID: 19897132.

21. Lee C, Lamart S, Moroz BE. Computational lymphatic node models in pediatric and adult hybrid phantoms for radiation dosimetry. *Phys Med Biol.* 2013;**58**(5):N59-82. doi: 10.1088/0031-9155/58/5/N59. PubMed PMID: 23391692. PubMed PMCID: PMC3878984.

22. Tapiovaara M, Lakkisto M and Servomaa A. PCXMC: a PC-based Monte Carlo program for calculating patient doses in medical x-ray examinations. Report STUK-A139; Helsinki, Finland: Finnish Centre for Radiation and Nuclear Safety Authority; 1997.

23. Ahnesjö A. Collapsed cone convolution of radiant energy for photon dose calculation in heterogeneous media. *Med Phys.* 1989;**16**(4):577-92. doi: 10.1118/1.596360. PubMed PMID: 2770632.

24. McNutt T. Dose calculations: collapsed cone convolution superposition and delta pixel beam. Pinnacle White Paper No. 4535 983 02474; Netherlands: Philips Medical System; 2002.

25. Wilke L, Andratschke N, Blanck O, et al. ICRU report 91 on prescribing, recording, and reporting of stereotactic treatments with small photon beams: Statement from the DEGRO/DGMP working group stereotactic radiotherapy and radiosurgery. *Strahlenther Onkol.* 2019;**195**(3):193-8. doi: 10.1007/s00066-018-1416-x. PubMed PMID: 30649567.

26. Ding GX, Munro P. Radiation exposure to patients from image guidance procedures and techniques to reduce the imaging dose. *Radiother Oncol.* 2013;**108**:91-98. doi: 10.1016/j.radonc.2013.05.034. PubMed PMID: 23830468.

27. Stock M, Palm A, Altendorfer A, Steiner E, Georg D. IGRT induced dose burden for a variety of imaging protocols at two different anatomical sites. *Radiother Oncol.* 2011;**102**:355-63. doi: 10.1016/j.radonc.2011.10.005. PubMed PMID: 22098793.

28. Nelson AP, Ding GX. An alternative approach to account for patient organ doses from imaging guidance procedures. *Radiother Oncol.* 2014;**112**:112-8. doi: 10.1016/j.radonc.2014.05.019. PubMed PMID: 25023041.

29. Murphy MJ, Balter J, Balter S, et al. The management of imaging dose during image-guided radiotherapy: report of the AAPM Task Group 75. *Med Phys.* 2007;**34**(10):4041-63. doi: 10.1118/1.2775667. PubMed PMID: 17985650.